AIP | Applied Physics Letters

Meandering of overgrown v-shaped defects in epitaxial GaN layers

P. H. Weidlich, M. Schnedler, V. Portz, H. Eisele, R. E. Dunin-Borkowski, and Ph. Ebert

Citation: Applied Physics Letters **105**, 012105 (2014); doi: 10.1063/1.4887372
View online: http://dx.doi.org/10.1063/1.4887372
View Table of Contents: http://scitation.aip.org/content/aip/journal/apl/105/1?ver=pdfcov
Published by the AIP Publishing

Meandering of overgrown v-shaped defects in epitaxial GaN layers

P. H. Weidlich,[1] M. Schnedler,[1] V. Portz,[1] H. Eisele,[2] R. E. Dunin-Borkowski,[1] and Ph. Ebert[1,a)]
[1]*Peter Grünberg Institut, Forschungszentrum Jülich GmbH, 52425 Jülich, Germany*
[2]*Institut für Festkörperphysik, Technische Universität Berlin, Hardenbergstr. 36, 10623 Berlin, Germany*

(Received 6 May 2014; accepted 25 June 2014; published online 8 July 2014)

The meandering of v-shaped defects in GaN(0001) epitaxial layers is investigated by cross-sectional scanning tunneling microscopy. The spatial position of v-shaped defects is mapped on $(10\bar{1}0)$ cleavage planes using a dopant modulation, which traces the overgrown growth front. Strong lateral displacements of the apex of the v-shaped defects are observed. The lateral displacements are suggested to be induced by the meandering of threading dislocations present in the v-shaped defects. The meandering of the dislocation is attributed to interactions with inhomogeneous strain fields. © *2014 AIP Publishing LLC*. [http://dx.doi.org/10.1063/1.4887372]

The application of group III-nitride semiconductors in highly efficient light emitter devices with a spectral range from ultraviolet to green progressed extremely fast.[1] Nevertheless, these materials are not well understood yet. In particular, defects play a critical role and the types of defects found in group III-nitrides are usually not present in conventional semiconductors in relevant concentrations. The importance of defects arises from the lack of large commercially available bulk substrates.[2,3] Hence, the epitaxial device structures have to be deposited on lattice-mismatched and thermal-mismatched substrates or on pseudo substrates which themselves were nucleated on mismatched substrates.[4] In both cases, the mismatch induces dislocations and other defects in high concentrations, which need to be reduced for improved optoelectronic properties.[1,5,6] Therefore, large efforts were made primarily in order to reduce the concentration of the threading dislocations by influencing their line direction by, e.g., epitaxial lateral overgrowth, patterning with semipolar facets, and/or interlayers.[7–17]

Some of the threading dislocations do, however, still continue to propagate along growth direction, penetrating through the whole epitaxial layers. Such threading dislocations as well as dislocations which can nucleate during growth instabilities, may give rise to three-dimensional inverted pyramidal pits (also called v-shaped defects), which occur at the intersection points of dislocations on the growth surface.[18–21] After overgrowth, the inverted pyramidal pits form three-dimensional v-shaped defects extending along growth direction.[18–23] The v-shaped defects introduce deep traps[23] and interact with the dislocations in their vicinity during overgrowth, reducing the dislocation concentration.[24] Hence, it is important to understand how the v-shaped defects propagate through the epitaxial layers during (over)growth.

In this Letter, we investigate the spatial meandering of v-shaped defects in GaN(0001) epitaxial layers grown along the *c*-direction using cross-sectional scanning tunneling microscopy (STM). We demonstrate that the v-shaped defects have an average orientation along the *c*-growth direction, but lateral jumps of up to 0.7 μm occur. This pronounced meandering of the v-shaped defects is attributed to a meandering of dislocations around which the v-shaped defects form.

In order to visualize overgrown v-shaped defects in cross-sectional STM (XSTM), we utilize an *n*-type doping modulation along the *c*–(growth) direction within the epitaxial GaN layers.[23] The doping modulation used in our samples is similar to that in Ref. 25 but with different thicknesses of the layers. This doping modulation is visible in XSTM images (Ref. 25) and is used to identify the positions of v-shaped defects after overgrowth by pure GaN. STM is perfectly suited to image shallow potential fluctuations over large fields of view, since the tunnel current is extremely sensitive to small changes of the Fermi energy (or potential).[26] In addition, the STM allows large scan ranges enabling the investigation of potential modulations and extended defects over up to several tenths of micrometers. These advantages provide the most direct access to extended v-shaped defects in pure GaN epitaxial layers in comparison to other microscopic methods as discussed in more detail later.

For our cross-sectional experiments, the samples were cleaved in ultrahigh vacuum (1×10^{-8} Pa) along a *m*-plane [$(10\bar{1}0)$ plane]. The cleavage opens a clean and adsorbate-free cross-sectional view of the overgrown epitaxial GaN layers.[27] For the XSTM measurements, we used electrochemically etched tungsten tips.

Figure 1(a) shows a constant-current XSTM image of a typical overgrown v-shaped defect exposed at a cross-sectional GaN$(10\bar{1}0)$ cleavage surface. The [0001] growth direction is toward the right side of this cross-sectional STM image, showing the empty density of states. The cleavage surface exhibits terraces separated primarily by monoatomic steps. Some steps abruptly terminate at dislocations intersecting the cleavage surface (marked by circles in Fig. 1(a)).[28–32] Superimposed on the stepped surface, a roughly periodical contrast change arising from a doping modulation can be discerned showing up as darker contrast. The orientation of the doping modulation exhibits sharp v-shaped cross-sections marked by v-shaped dashed lines in each period of the doping modulation (with an average periodicity length x_{mod}). These v-shaped corners, visible in the two-dimensional cross-section of the GaN epitaxial layers, arise from overgrown three-dimensional inverted pyramidal pit structures at the growth

a)Electronic mail: p.ebert@fz-juelich.de

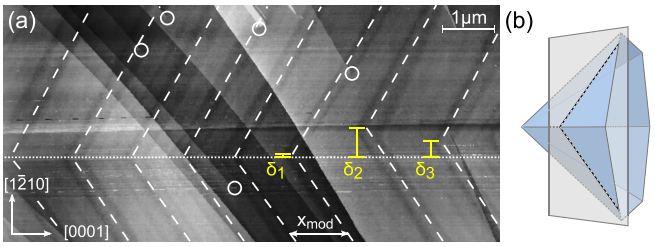

FIG. 1. (a) STM image of a cleaved $(10\bar{1}0)$ surface of a modulation-doped GaN epitaxial layer showing a cross-section through an overgrown v-shaped defect. The v-shaped structure and its corners are indicated by the dashed lines. The lateral displacements marked by δ_1 to δ_3 indicate a meandering of the v-shaped corners. Superimposed on the contrast of the doping modulation, the surface exhibits cleavage steps and, at their end points, dislocation lines intersecting the cleavage surface (marked by circles). The constant-current image shows the empty density of states acquired at a voltage of +4.0 V and 100 pA of set current. (b) Schematic of the cross-sectional off-center cut indicated by the gray plane through a v-shaped defect. The white and black dashed lines indicate the cross-section of the v-shaped defect as seen in the STM image.

surface delimited by six $\{11\bar{2}2\}$ inclined growth facets (schematically shown in Fig. 1(b)).[23] The overgrown pits lead to v-shaped defects extending along the c direction. Note, the cross-sectional cleavage planes cut through the v-shaped defects typically at some off-center position. Hence, the edge between two adjacent $\{11\bar{2}2\}$ planes leads to the observed v-shaped corners in the $(10\bar{1}0)$ cross section in the STM images.

The important point is the determination of the spatial positions of the individual v-shaped corners in the two dimensional cross-sections with progressing growth. The layers at the left hand side of Fig. 1(a) were grown first, with the growth direction toward the right hand side. Hence, the location within the epitaxial layer in Fig. 1(a) yields the spatial position of the v-shaped corners as a function of the progressing growth. The v-shaped corners in each layer form a line extending along the growth direction as indicated by a dotted straight line in Fig. 1(a). This is consistent with the extension of the v-shaped defects along the c direction. However, at a closer look the v-shaped corners suddenly deviate from the dotted line by lateral displacements along the $[1\bar{2}10]$ direction labeled δ_1, δ_2, and δ_3. Lateral displacements δ from the average position of the v-shaped corner of up to 0.5 μm were observed. Despite the existence of those lateral displacements, the angle of the cross sectioned inclined facets of the v-shaped defects is not changed. Hence, the three-dimensional geometrical shape (i.e., an inverted pyramidal shape delimited by six $\{11\bar{2}2\}$ planes with an opening angle on the cross-sectional m-plane of $\alpha = 101.8°$)[23] of the v-shaped defect is not changed. This suggests that the position of the center of the overgrown v-shaped defects or of the inverted pyramidal pits at the growth surface shifts spatially perpendicular to the growth direction. This leads to a spatial fluctuation of the edge between two adjacent $\{11\bar{2}2\}$ inclined facets of the inverted pyramidal pit. Hence, the lateral displacements of the v-shaped corners observed in the cross-sectional STM images trace the (in $(10\bar{1}0)$ direction) projected spatial shifts of the center of the v-shaped defect with progressing growth.

In order to quantify the degree of spatial shifts of the v-shaped defects, we measured the lateral displacements of the v-shaped corner within every doping modulation period. For this purpose, several v-shaped defects were analyzed. The distortions due to the scanning tube of the STM have been corrected in every STM image to allow an accurate measurement of the distances and angles.[33] The resulting distribution of the lateral displacements δ along the $[1\bar{2}10]$ direction from the average position is shown in Fig. 2(a). Note, the lateral displacements are geometrically limited, since successively grown layers need to have their v-shaped apex always within the inclined v-shaped facets of the previously grown layer. Otherwise, the v-shaped defect would terminate and another one would be nucleated at a neighboring position. Hence, the lateral displacement is measured in units of the maximal lateral displacement δ_{max}, which is given by half of the width of the cross-sectioned v-shaped defect $\delta_{max} = x_{mod} \times \tan\alpha \approx 1.2\,\mu$m at a height of one average modulation period x_{mod} of $\approx 1\,\mu$m.

The distribution of the lateral displacements in Fig. 2(a) is symmetrical and centered around a lateral displacement $\delta = 0$. This indicates that on average the overgrown v-shaped

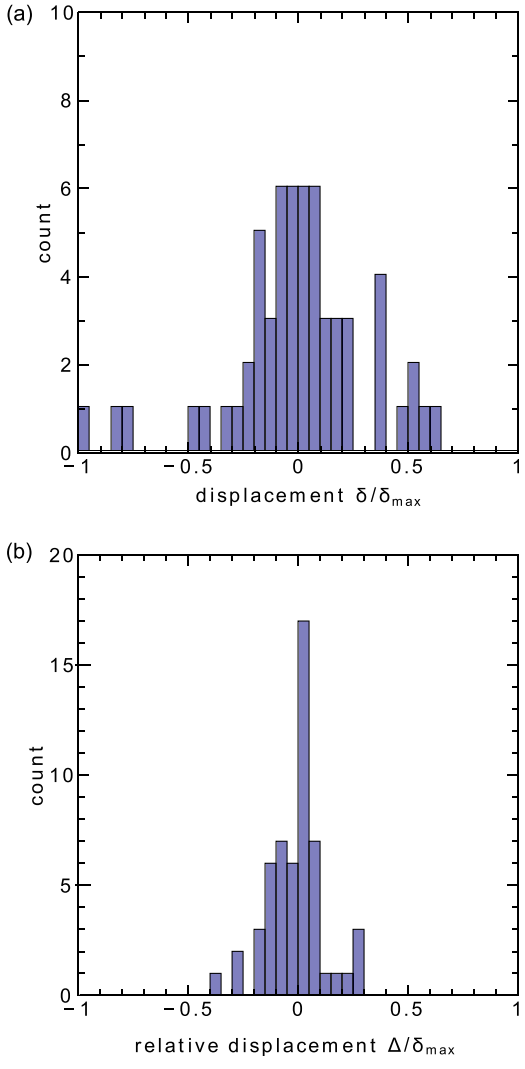

FIG. 2. (a) Frequency distribution of the lateral displacements δ along the $[1\bar{2}10]$ direction of the positions of v-shaped corners from the average position in units of $\delta_{max} \approx 1.2\,\mu$m. The distribution is centered along the c-direction (equal to displacement 0), but with a large width. (b) Frequency distribution of the jumps in lateral displacement $\Delta_i = \delta_i - \delta_{i-1}$ within one modulation period. Jumps in lateral displacements of up to 0.5 μm occur.

defects propagate along c growth direction. The width of the distribution of $0.27 \times \delta_{\max} \approx 0.32\mu$m indicates a significant meandering within the maximum field of view of 20 μm used in the measurements. The frequency distribution of the jumps in the lateral displacement $\Delta_i = \delta_i - \delta_{i-1}$ within one period [Fig. 2(b)] shows that spatial jumps of up to 0.5 μm occur within one modulation period. Assuming a constant bending of the center line of the v-shaped defect, i.e., the position of the apex of the overgrown inverted pyramidal pit structure, the maximum bending angle in the $(10\bar{1}0)$ projection would be in the order of 26°. Hence, v-shaped defects in GaN epitaxial layers exhibit a pronounced meandering.

At this stage, we discuss the origin of the observed meandering of the v-shaped defects. In an ideal dislocation-free GaN material no strain field is present and hence a v-shaped defect should not undergo any lateral displacements with progressing growth. The spatial position would be only determined by the growth speeds on the different facets. Since the six delimiting $\{11\bar{2}2\}$ facets should have equal growth speeds, the inverted pyramidal pit at the growth surface should either deepen or flatten out, depending on the relative growth speed along the $\{11\bar{2}2\}$ and $\{0001\}$ directions. However, in hydride vapor phase epitaxy grown GaN inverted pyramidal v-shaped pits are known to form at growth instabilities, such as impurities, droplets, and/or defects.[22,34] These induce strain fields. Hence, it can be expected that growth instabilities act as nucleation centers of dislocations around which the v-shaped defects form. Thus, the assumption of strain free material, as made above, is not fulfilled. During progressing growth, the v-shaped inverted pyramidal pit is overgrown and its apex should follow the intersection point of the dislocation at the growth surface at any moment during growth. Therefore, we need to discuss the line directions of the dislocations.

There are three types of threading dislocations in GaN epitaxial layers: First, initially pure edge dislocations with $\frac{a}{3}\langle 11\bar{2}0\rangle$-type Burgers vectors ($a$-type dislocations) are usually bent toward the non-polar directions[9,24,35–37] since their lowest energy state is for a 90° bending.[38] Second, dislocations with an $\frac{a}{3}\langle 11\bar{2}\ \frac{\pm 3c}{a}\rangle$ Burgers vector (components along the a- and c-directions, $a+c$-type dislocations) have a significantly lower concentration[39–41] due to the higher energy related to the longer Burgers vector.[42] Third, pure screw dislocations with a Burgers vector of $\pm c[0001]$ (c-type dislocations) exist. Their energy should be lowest with a line direction along the c direction.[38] Hence, they are likely to propagate through the entire epitaxial layer during overgrowth, always intersecting with the growth surface.[29] It can be expected that this type of dislocation is present at the center of the v-shaped defects.

Although the energy of c-type screw dislocations with $\pm c[0001]$ Burgers vector should be lowest with a line direction parallel to the Burgers vector (or c direction), the dislocation line may deviate from this preferred orientation. Thermally induced kinks of the dislocation line can increase the entropy and hence lower the free energy, an effect relevant especially at high temperatures, such as those occurring during GaN growth.[43] This may induce a meandering of a dislocation around its preferred line direction. However, the large jumps in the lateral displacement of up to 0.5 μm observed here are unlikely to be explainable solely based on entropy effects.

In order to explain large lateral displacements, we need to consider the glide and interactions of dislocations. First, c-type screw dislocations with $\pm c[0001]$ Burgers vector glide on the densest packed non-polar plane, i.e., $(10\bar{1}0)$, in $\langle 11\bar{2}0\rangle$ direction. This slip system is compatible with the observed meandering. Second, threading dislocations will interact with strain fields in the material, which induce gliding of dislocations. Since dislocations were found to form agglomerations in GaN epitaxial layers with densities ranging from $0^{+4\times10^6}_{-0}$ to $(6\pm2)\times10^7\,\mathrm{cm}^{-2}$ (considering a $5\times5\,\mu\mathrm{m}^2$ mesh),[24] the magnitude and orientation of the surrounding strain fields will fluctuate and hence the degree of interaction. For example, it has been shown by electron tomography that threading dislocations interact with bundles of dislocations in GaN.[44,45] Thus, depending on the local distribution of strain fields, the force on the dislocation line can be expected to fluctuate along the c direction and hence the amount of slip of the different sections of the dislocation line. Hence, fluctuations in the strain fields may indeed induce a meandering of screw dislocations.

If the material contains strong gradients in the strain field due to mismatched layers, such as in InGaN/GaN superlattices, the gradients of the strain field due to the superlattice may push the dislocation to align with the superlattice-induced strain field gradient. In our case, the Si modulation doping induces a strain field gradient comparable to the strain introduced by only ≈0.1% of In in GaN, as calculated using the Si and In induced lattice constant changes of GaN.[25] Hence, the doping induced strain field is negligible, here.

A meandering of a screw dislocation induces spatial shifts of the intersection point of the dislocation line at the growth surface. The apex of the inverted pyramidal pit at the growth surface can be expected to follow these spatial shifts. Hence, with progressing growth, the apex of the overgrown v-shaped defect meanders too, tracing the dislocation line. In the cross-sectional view, the meandering of the apex of the v-shaped defect shows up as lateral displacements of the v-shaped corners as observed in Fig. 1(a). Thus, the measured pronounced displacements of the v-shaped corners in the cross-sectional STM images suggest that the dislocation line exhibits a significant bending reaching in $(10\bar{1}0)$ projection the order of 26°.

It would desirable to simultaneously image the dislocation(s) within a v-shaped defect and the v-shaped defect itself. However, this task is extremely tempting: The main drawbacks are that STM cannot detect dislocations lying entirely in the bulk material.[24,32] On the other hand, conventional transmission electron microscopy (TEM) cannot image the shallow doping Si modulation in pure GaN due to the small Z difference of Si and Ga. Furthermore, the doping modulation induces a potential modulation smaller than 10 meV, as derived using Ref. 25. Detecting this by electron holography in TEM is extremely tempting due to the need of a large sample view of several μm^2 with well defined and known sample thickness and due to systematic errors limiting the accuracy of the potential determination to the range of 100–200 meV.[46,47] Finally, the sample preparation and the

high energy electron beam lead to damaged layers as thick as 100 nm which modify the potential by introducing defect states.[47] Thus, at present, one can only image the dislocations or the v-shaped defects separately.

In conclusion, cross-sectional scanning tunneling microscopy of GaN epitaxial layers showed that overgrown v-shaped defects exhibit a pronounced meandering around their average orientation in *c* (growth) direction. The meandering is suggested to arise from the tracing of a meandering threading dislocation at the center of the v-shaped defect. The interaction of the dislocation with the surrounding inhomogeneous strain field is related to the meandering of the dislocation line. A quantitative analysis of the lateral displacements of the v-shaped defects allows to estimate the degree of bending of the dislocation line.

The authors thank the Deutsche Forschungsgemeinschaft for financial support under Grant Nos. Eb197/5-1 and Ei788/2-1 and K.-H. Graf for technical support.

[1]S. Nakamura, MRS Bull. **34**, 101 (2009).
[2]I. Grzegory, B. Łucznik, M. Boćkowski, and S. Porowski, J. Cryst. Growth **300**, 17 (2007).
[3]S. Porowski, J. Cryst. Growth **189–190**, 153 (1998).
[4]P. Gibart, Rep. Prog. Phys. **67**, 667 (2004).
[5]Y. Y. Enya, Y. Yoshizumi, T. Kyono, K. Akita, M. Ueno, M. Adachi, T. Sumitomo, S. Tokuyama, T. Ikegami, K. Katayama, and T. Nakamura, Appl. Phys. Express **2**, 082101 (2009).
[6]S. E. Bennett, Mater. Sci. Technol. **26**, 1017 (2010).
[7]A. Usui, H. Sunakawa, A. Sakai, and A. A. Yamaguchi, Jpn. J. Appl. Phys., Part 2 **36**, L899 (1997).
[8]O.-H. Nam, M. D. Bremser, T. S. Zheleva, and R. F. Davis, Appl. Phys. Lett. **71**, 2638 (1997).
[9]P. Vennéguès, B. Beaumont, V. Bousquet, M. Vaille, and P. Gibart, J. Appl. Phys. **87**, 4175 (2000).
[10]K. Hiramatsu, K. Nishiyama, M. Onishi, H. Mizutani, M. Narukawa, A. Motogaito, H. Miyake, Y. Iyechika, and T. Maeda, J. Cryst. Growth **221**, 316 (2000).
[11]A. Krost and A. Dadgar, Phys. Status Solidi A **194**, 361 (2002).
[12]A. Dadgar, M. Poschenrieder, J. Blasing, K. Fehse, A. Diez, and A. Krost, Appl. Phys. Lett. **80**, 3670 (2002).
[13]K. Motoki, T. Okahisa, S. Nakahata, N. Matsumoto, H. Kimura, H. Kasai, K. Takemoto, K. Uematsu, M. Ueno, Y. Kumagai, A. Koukitu, and H. Seki, J. Cryst. Growth **237–239**, 912 (2002).
[14]V. Wagner, O. Parillaud, H. J. Bühlmann, M. Ilegems, S. Gradeçak, P. Stadelmann, T. Riemann, and J. Christen, J. Appl. Phys. **92**, 1307 (2002).
[15]K. Pakuła, R. Bożek, J. Baranowski, J. Jasinski, and Z. Liliental-Weber, J. Cryst. Growth **267**, 1 (2004).
[16]S. Bohyama, H. Miyake, K. Hiramatsu, Y. Tsuchida, and T. Maeda, Jpn. J. Appl. Phys., Part 2 **44**, L24 (2005).
[17]M. Ali, A. Romanov, S. Suihkonen, O. Svensk, S. Sintonen, M. Sopanen, H. Lipsanen, V. Nevedomsky, N. Bert, M. Odnoblyudov, and V. Bougrov, J. Cryst. Growth **344**, 59 (2012).
[18]Z. Liliental-Weber, Y. Chen, S. Ruvimov, and J. Washburn, Phys. Rev. Lett. **79**, 2835 (1997).
[19]Y. Chen, T. Takeuchi, H. Amano, I. Akasaki, N. Yamada, Y. Kaneko, and S. Y. Wang, Appl. Phys. Lett. **72**, 710 (1998).
[20]T. Paskova, E. M. Goldys, R. Yakimova, E. B. Svedberg, A. Henry, and B. Monemar, J. Cryst. Growth **208**, 18 (2000).
[21]X. H. Wu, C. R. Elsass, A. Abare, M. Mack, S. Keller, P. M. Petroff, S. P. DenBaars, J. S. Speck, and S. J. Rosner, Appl. Phys. Lett. **72**, 692 (1998).
[22]J. Weyher, B. Łucznik, I. Grzegory, J. Smalc-Koziorowska, and T. Paskova, J. Cryst. Growth **312**, 2611 (2010).
[23]P. H. Weidlich, M. Schnedler, H. Eisele, U. Strauß, R. Dunin-Borkowski, and Ph. Ebert, Appl. Phys. Lett. **103**, 062101 (2013).
[24]P. H. Weidlich, M. Schnedler, H. Eisele, R. Dunin-Borkowski, and Ph. Ebert, Appl. Phys. Lett. **103**, 142105 (2013).
[25]H. Eisele, L. Ivanova, S. Borisova, M. Dähne, M. Winkelnkemper, and Ph. Ebert, Appl. Phys. Lett. **94**, 162110 (2009).
[26]S. Landrock, Y. Jiang, K. H. Wu, E. G. Wang, K. Urban, and Ph. Ebert, Appl. Phys. Lett. **95**, 072107 (2009).
[27]H. Eisele and Ph. Ebert, Phys. Status Solidi RRL **6**, 359 (2012).
[28]G. Cox, D. Szynka, U. Poppe, K. H. Graf, K. Urban, C. Kisielowski-Kemmerich, J. Krüger, and H. Alexander, Phys. Rev. Lett. **64**, 2402 (1990).
[29]A. R. Smith, V. Ramachandran, R. M. Feenstra, D. W. Greve, M.-S. Shin, M. Skowronski, J. Neugebauer, and J. E. Northrup, J. Vac. Sci. Technol., A **16**, 1641 (1998).
[30]S. Vézian, J. Massies, F. Semond, N. Grandjean, and P. Vennéguès, Phys. Rev. B **61**, 7618 (2000).
[31]Ph. Ebert, C. Domke, and K. Urban, Appl. Phys. Lett. **78**, 480 (2001).
[32]Ph. Ebert, L. Ivanova, S. Borisova, H. Eisele, A. Laubsch, and M. Dähne, Appl. Phys. Lett. **94**, 062104 (2009).
[33]M. Schnedler, P. H. Weidlich, V. Portz, D. Weber, R. E. Dunin-borkowski, and Ph. Ebert, Ultramicroscopy **136**, 86 (2014).
[34]E. Richter, U. Zeimer, S. Hagedorn, M. Wagner, F. Brunner, M. Weyers, and G. Tränkle, J. Cryst. Growth **312**, 2537 (2010).
[35]A. Sakai, H. Sunakawa, and A. Usui, Appl. Phys. Lett. **73**, 481 (1998).
[36]E. Feltin, B. Beaumont, P. Vennéguès, M. Vaille, P. Gibart, T. Riemann, J. Christen, L. Dobos, and B. Pécz, J. Appl. Phys. **93**, 182 (2003).
[37]A. E. Romanov, P. Fini, and J. S. Speck, J. Appl. Phys. **93**, 106 (2003).
[38]S. Gradeçak, P. Stadelmann, V. Wagner, and M. Ilegems, Appl. Phys. Lett. **85**, 4648 (2004).
[39]X. H. Wu, L. M. Brown, D. Kapolnek, S. Keller, B. Keller, S. P. DenBaars, and J. S. Speck, J. Appl. Phys. **80**, 3228 (1996).
[40]N. Grandjean, J. Massies, P. Vennéguès, M. Leroux, F. Demangeot, M. Renucci, and J. Frandon, J. Appl. Phys. **83**, 1379 (1998).
[41]Y. Xin, S. J. Pennycook, N. D. Browning, P. D. Nellist, S. Sivananthan, F. Omnes, B. Beaumont, J. P. Faurie, and P. Gibart, Appl. Phys. Lett. **72**, 2680 (1998).
[42]D. Hull and D. J. Bacon, *Introduction to Dislocations*, 5th ed. (Elsevier, 2011).
[43]J. Friedel, Philos. Mag. **45**, 271 (1982).
[44]J. S. Barnard, J. Sharp, J. R. Tong, and P. A. Midgley, Science **313**, 319 (2006).
[45]J. S. Barnard, J. Sharp, J. R. Tong, and P. A. Midgley, Philos. Mag. **86**, 4901 (2006).
[46]W. D. Rau, P. Schwander, F. H. Baumann, W. Höppner, and A. Ourmazd, Phys. Rev. Lett. **82**, 2614 (1999).
[47]A. C. Twitchett-Harrison, T. J. V. Yates, S. B. Newcomb, R. E. Dunin-Borkowski, and P. A. Midgley, Nano Lett. **7**, 2020 (2007).